The Monte Carlo Method: Versatility Unbounded in a Dynamic Computing World
Chattanooga, Tennessee, April 17-21, 2005, on CD-ROM, American Nuclear Society, LaGrange Park, IL (2005)

GEANT4 SIMULATION OF AN ACCELERATOR HEAD FOR INTENSITY MODULATED RADIOTHERAPY

F. Foppiano
National Cancer Research Institute (IST)
Largo Rosanna Benzi10, 16132 Genova - Italy
franca.foppiano@istge.it.

B. Mascialino, M.G. Pia and M. Piergentili
Italian Institute for Nuclear Research (INFN)
via Dodecaneso 33, 16146 Genova -Italy
Barbara.Mascialino@ge.infn.it; MariaGrazia.Pia@ge.infn.it; Michela.Piergentili@ge.infn.it

ABSTRACT

We present a Geant4-based application for the simulation of the absorbed dose distribution given by a medical linac used for intensity modulated radiation therapy (IMRT). The linac geometry is accurately described in Monte Carlo code using the accelerator's manufacturer's specifications. The flexible design of this object-oriented system allows for an easy configuration of the geometry of the treatment head for various types of medical accelerators used in clinical practice.

The precision of the software system relies on the application of Geant4 Low Energy Electromagnetic models, extending the treatment of electron and photon interaction down to low energies for precise dosimetry.

The capability of the software to evaluate dose distribution has been verified by comparison with measurements in water phantom; the comparisons were performed for percent depth dose (PDD) and for flatness at 15, 50 and 100 mm depth for various field size, for a 6 MV electron beam. The source-surface distance (SSD) was 100 cm. We show the comparisons between simulation results and experimental measurements.

The code is fully parallelized, allowing to achieve the high statistics Monte Carlo production required fastly. The parallelization scheme adopted allows to run the code trasparently either in a local computing farm or with geografically distributed resources, such as a computing GRID.

This software system is released to the public as an open source software system, for the benefit of the scientific community.

Key Words: IMRT, Geant4, Radiotherapy

1 INTRODUCTION

The development of advanced techniques in radiotherapy, such as intensity modulation, brings about the need for more sophisticated and precise methods to calculate dose distributions.

In particular, Intensity Modulated Radiation Therapy (IMRT) involves a series of small fields, to obtain a specific treatment, with a complex dose distribution, for an individual patient.

The most sophisticated commercial treatment planning system use some approximation to reduce calculation time, but these deficiencies are not negligible in a modern technique as IMRT. A Monte Carlo method, which accounts for non equilibrium situations, seems to be a good system to verify a treatment plan.

The project described in this paper developed a dosimetric system, based on a Monte Carlo method, which calculates accurately dose distributions for IMRT.

2 MATERIALS AND METHODS

We developed a Geant4 application, which simulates the linear accelerator head used for IMRT at the National Institute of Cancer Research Institute in Genova.

2.0.1 Geometrical model

The components in the simulated LINAC head were the following: target, primary collimator, vacuum windows, flattening filter, ion chamber, mirror, two pair of jaws, multileaf collimator and the phantom. Each pair of jaws can be rotated through an axis that is perpendicular to the beam axis. The user can select the position of each jaw and of every single leaf of the multileaf collimator.

The powerful tools provided by Geant4 allow us to simulate the geometrical shape of each component of the LINAC head with high precision; for instance, we model the rounded leaf tips and the lateral step of leaf in the multileaf collimator, and the real shape of the flattening filter according to manufacturer's directions.

The simulated detector is a phantom; it is made of water or plexiglass according to the corresponding experimental setup. The phantom was divided in voxels, in which we collected the energy deposit to calculate the relative dose absorbed. In the case of squared fields the phantom was made of water, in the case of the intensity modulated fields the phantom was made of plexiglass.

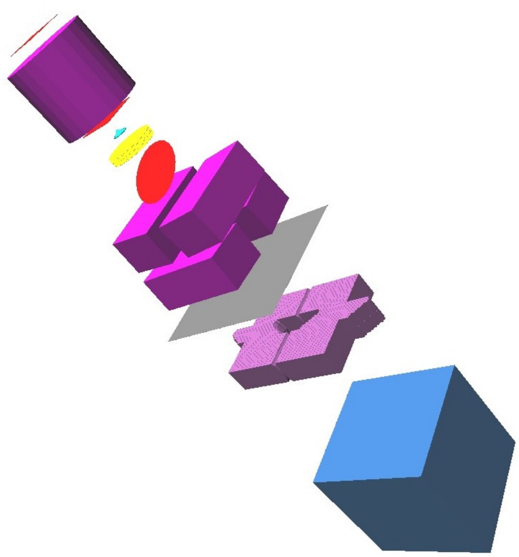

Figure 1: Image produced with the simulation system, representing the head of the LINAC and the water phantom.

Figure 1 shows all the modelled components of the LINAC head.

Geant4 offers several visualization tools, which allow us to verify the correctness of the geometrical model. The Geant4 medical linac application was developed following a rigorous software process, which guarantees the quality and reliability of the product. This system is based

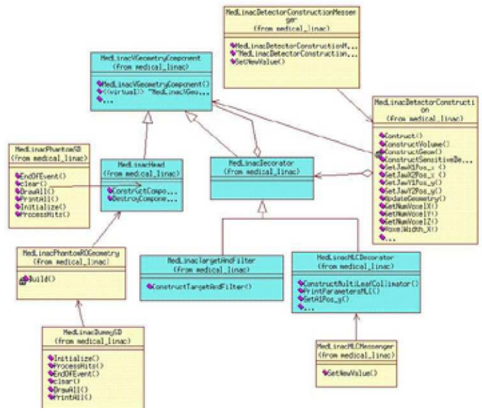

Figure 2: Class diagram representing the design pattern Decorator used in the model of the LINAC's head.

on the object oriented technology and on a sound architecture.

In the clinical practice, the setup of the head can be changed between two treatments: the physicist can change the energy of the beam or the position of some collimators, and can change or replace some components. In the simulated head the physicist should be able to make the same actions; to this purpose the geometry design adopts a Decorator pattern **??** to configure the treatment head dynamically.

Figure 2 shows the class diagram of geometry design.

2.0.2 Physical model

Specifically for our application, of particular interest is the Low Energy Package [2] in Geant4, developed to extend electromagnetic interaction of particles with matter down to very low energy: 250 eV for electrons and photons. This package allows us to calculate with high precision the energy deposit in radiotherapic application.

The physical processes implemented in the simulation are : Rayleigh effect, photoelectric effect, Compton effect, and pair production for photons; ionization, Bremsstrahlung, multiple scattering and annihilation for electrons and positrons. We have assumed a Gaussian distribution for energy and momentum of the primary electrons.

2.0.3 Analysis

The analysis component of this system is based on the AIDA analysis tool. This component collects all the data about the dose distribution in several histograms, which the user can elaborate to obtain percent depth dose and lateral dose distributions.

2.1 Experimental measurements

The measurements of both depth dose curves and lateral dose profiles for the squared fields were made using an ion chamber (31002 Semiflex, PTW, Freiburg Germany) with an active volume of $0.125\ \mathrm{cm}^3$ and a cavity diameter of 0.55 cm. The ion chamber was mounted on a computer controlled scanning system (MP3-System, PTW, Freiburg Germany). The uncertainty of the position accuracy of the scanning system provided by the manufacturer was ± 0.1 mm. All the measurements were obtained at a source-surface distance (SSD) of 100 cm. The effective point of measurement for the ion chamber was taken to be $0.60 \mathrm{r_{cav}}$, where $\mathrm{r_{cav}}$ is the cavity radius of the chamber, consistent with the International Atomic Energy Agency (IAEA) protocol [4]. The estimated total uncertainty of an ionization measurement at a given depth was 0.5%, deriving from the positioning reproducibility of the ion chamber and short term fluctuations of the chamber, electrometer, air pressure and temperature, during the time frame of one scan. The estimated total uncertainty of a relative dose measurement was taken to be 1.8%; this estimation takes in account the relative uncertainty on the calibration of the dosimeter, on the correction terms for influence quantities, on the beam quality correction, the long term stability of the dosimeter, on the dosimeter reading, the long term stability of user dosimeter and the establishment of reference conditions.

The measurements of absorbed dose in a plane, for the fields obtained with the multileaf collimator, were made using Kodak X-Omat V films and the film dosimetry system RIT113 with the scanner VXR-16 DosimetryPRO.

2.2 Normalization and comparison of data

Data concerning the depth-dose curves were normalized to their maximum value. Lateral profiles obtained with experimental measurements were normalized to the dose value on the beam axis, while the ones obtained with the software system were normalized to the mean value in the flat zone. Moreover in the specific case of the lateral profiles, we rebinned data in the central flat region, with the aim of reducing statistical fluctuations.

Statistical comparisons between experimental measurements and Geant4 simulations have been performed by means of a Goodness-of-Fit statistical toolkit [5], specialized in the comparison of data distributions. Among the ones available in the toolkit, we have selected the Kolmogorov-Smirnov [6] test. In the particular case of lateral dose profiles, we divided both experimental data and Geant4 simulation results in five regions of interest, having a relevance in the medical-physics domain: the central flat zone, the two high gradient regions and the tails; we tested the agreement between the two distributions within each of these regions of interest.

For any analysis performed, the confidence level was set to the value 0.05; a p-value higher than 0.05 led to the acceptance of the null hypothesis, stating the equivalence between reference data and Geant4 simulations.

3 RESULTS

In all the simulations, we reproduced with the dosimetric system the real experimental set-up, such as the position of the jaws and of every single leaf of the multileaf collimator, the energy of the beam, the source-surface distance and the material of the phantom.

3.1 Field 10x10 cm

We start this study from the 10x10 cm field, that is often used as a reference field to calculate relevant dosimetric quantities.

In Figure 3 we show the lateral dose profiles at 50 mm depth for the 10x10 cm field, with the 6 MV beam (SSD=100 cm). Table I shows the quantitative statistical results obtained in each

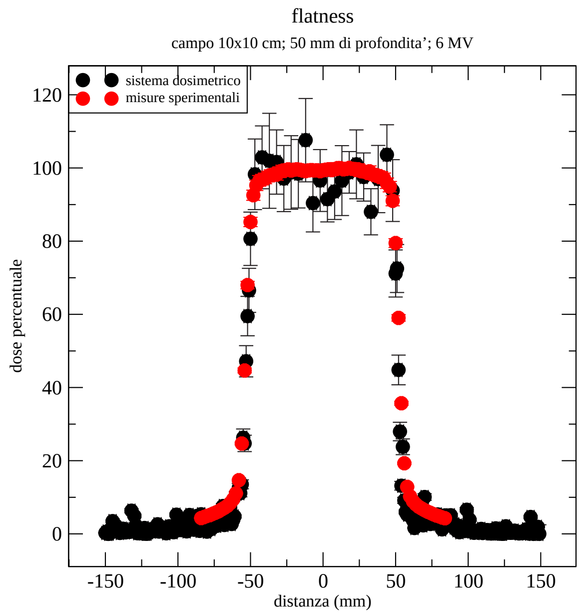

Figure 3: Lateral dose profiles at 50 mm depth, for the 10x10 cm field, with the 6 MV beam. The red symbols correspond to the experimental measurements, the dark symbols correspond to the Geant4 simulation.

region of interest: the first and the second columns indicate the region of interest under study, in the third column we reported the distance between the two distributions (Kolmogorov-Smirnov test statistics) and in the fourth column we listed the corresponding p-value. In any region considered, the Kolmogorov-Smirnov test pointed out a good agreement between experimental data and Geant4 simulations (p-values $>$ 0.05 in any case).

Table I: Results of the Kolmogorov-Smirnov test for the lateral dose profiles at of 50 mm depth, for the 10x10 cm field, with the 6 MV beam.

region of interest	range	distance	p-value
tail	-84, -60 mm	0.39	0.23
high gradient zone	-59, -48 mm	0.27	0.90
central flat zone	-47, 47 mm	0.43	0.19
high gradient zone	48, 59 mm	0.30	0.82
tail	60, 84 mm	0.40	0.10

In Figure 4 we show the lateral dose profiles at 100 mm depth, for the 10x10 cm field, with the 6 MV beam (SSD=100 cm). Table II shows the quantitative statistical results obtained in each region of interest: the first and the second columns indicate the region of interest under study, in

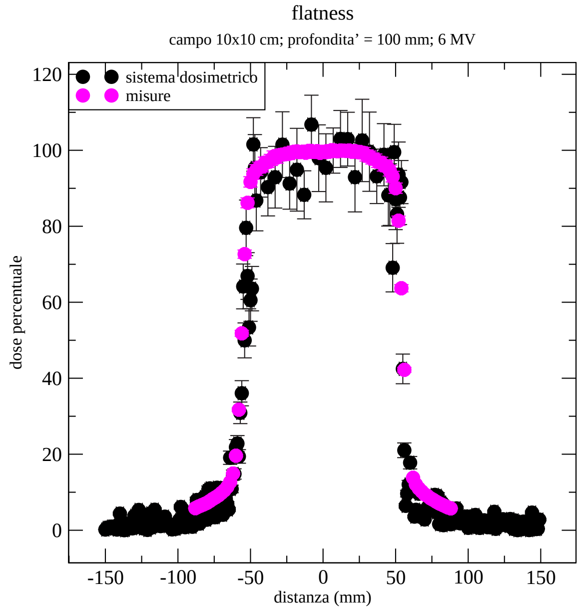

Figure 4: Lateral dose profiles at 100 mm depth, for the 10x10 cm field, with the 6 MV beam. The pink symbols correspond to the experimental measurements, the dark symbols correspond to the Geant4 simulation.

the third column we reported the distance between the two distributions (Kolmogorov-Smirnov test statistics) and in the fourth column we listed the corresponding p-value. In any region considered, the Kolmogorov-Smirnov test pointed out a good agreement between experimental data and Geant4 simulations (p-values > 0.05 in any case).

Table II: Results of the Kolmogorov-Smirnov test for the lateral dose profiles at 100 mm depth, for the 10x10 cm field, with the 6 MV beam.

region of interest	range	distance	p-value
tail	-84, -64 mm	0.43	0.25
high gradient zone	-63, -46 mm	0.33	0.60
central flat zone	-45, 50 mm	0.52	0.17
high gradient zone	51, 56 mm	0.52	0.65
tail	57, 84 mm	0.38	0.40

3.2 Field 5x5 cm

After the 10x10 cm field, we studied the 5x5 cm field, that have dimensions similar to the fields used in IMRT.

In Figure 5 we show the lateral dose profiles at 15 mm depth, for the 5x5 cm field, with the 6 MV beam (SSD=100 cm).

Table III shows the quantitative statistical results obtained in each region of interest: the first

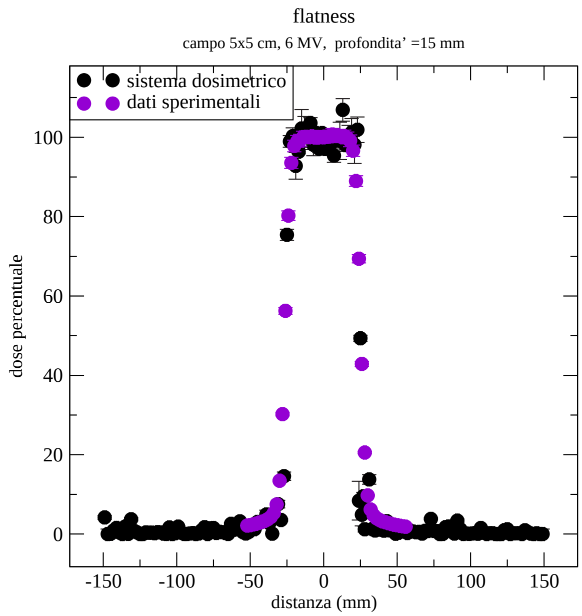

Figure 5: Lateral dose profiles at 15 mm depth, for the 5x5 cm field, with the 6 MV beam. The violet symbols correspond to the experimental measurements, the dark symbols correspond to the Geant4 simulation.

and the second columns indicate the region of interest under study, in the third column we reported the distance between the two distributions (Kolmogorov-Smirnov test statistics) and in the fourth column we listed the corresponding p-value. In any region considered, the Kolmogorov-Smirnov test pointed out a good agreement between experimental data and Geant4 simulations (p-values > 0.05 in any case).

Table III: Results of the Kolmogorov-Smirnov test for the lateral dose profiles at 15 mm depth, for the 5x5 cm field, with the 6 MV beam.

region of interest	range	distance	p-value
tail	-56, -35 mm	0.26	0.89
high gradient zone	-34, -22 mm	0.43	0.42
central flat zone	-21, 21 mm	0.38	0.08
high gradient zone	22, 32 mm	0.26	0.98
tail	33, 56 mm	0.57	0.13

In Figure 6 we show the lateral dose profiles at 100 mm depth, for the 5x5 cm field, with the 6 MV beam (SSD=100 cm). Table IV shows the quantitative statistical results obtained in each region of interest: the first and the second columns indicate the region of interest under study, in the third column we reported the distance between the two distributions (Kolmogorov-Smirnov test statistics) and in the fourth column we listed the corresponding p-value. In any region considered, the Kolmogorov-Smirnov test pointed out a good agreement between experimental data and Geant4 simulations (p-values > 0.05 in any case).

Table IV: Results of the Kolmogorov-Smirnov test for the lateral dose profiles at 100 mm depth, for the 5x5 cm field, with the 6 MV beam.

region of interest	range	distance	p-value
tail	-61, -35 mm	0.33	0.5
high gradient zone	-34, -26 mm	0.40	0.75
central flat zone	-25, 21 mm	0.32	0.24
high gradient zone	22, 32 mm	0.27	0.75
tail	33, 61 mm	0.21	0.91

3.3 Field 40x40 cm

We have started to study the 40x40 cm field, that can help us to determine if we have used the correct parameters characterizing the initial electron beam.

In Figure 7 we show the depth dose curves at 100 mm depth, for the 40x40 cm field, with the 6 MV beam (SSD=100 cm). Table V contains the results of the Kolmogorov-Smirnov test, the test demonstrate that the dosimetric system can simulate with great accuracy the experimental measurements.

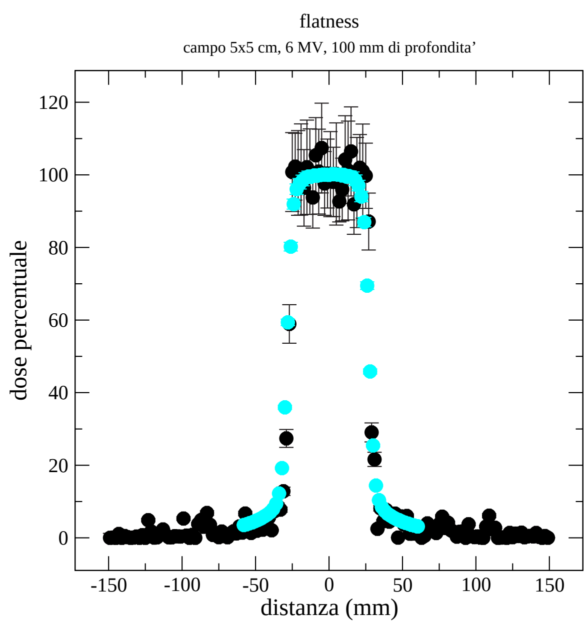

Figure 6: Lateral dose profiles at 100 mm depth, for the 5x5 cm field, with the 6 MV beam. The azure symbols correspond to the experimental measurements, the dark symbols correspond to the Geant4 simulation.

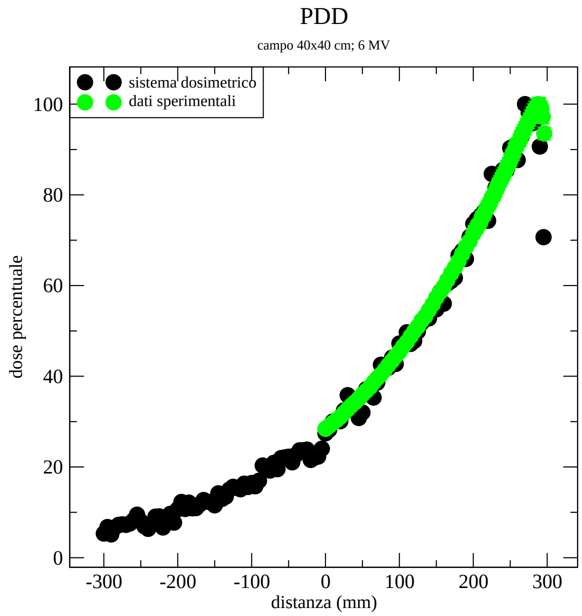

Figure 7: Depth dose distribution, for the 40x40 cm field, with the 6 MV beam. The green symbols correspond to the experimental measurements, the dark symbols correspond to the Geant4 simulation.

Table V: Results of the Kolmogorov-Smirnov test for the depth-dose curves, for the 40x40 cm field, with the 6 MV beam.

range	distance	p-value
0, 300 mm	0.005	1

3.4 Field obtained with intensity modulated beams

We studied an intensity modulated field used to treat a patient with prostate cancer. This field was obtained superimposing two fields shaped with the multileaf collimator.

Figure 8 shows the whole intensity modulated field; this figure illustrates the dose distribution in a plane, obtained with the simulation system.

In figure 8 we can appreciate the regions with different dose intensity, and we can see that the simulation system is able to reproduce the dose distribution, and in particular the dose interleaf transmission due to the rounded leaf tips.

4 CONCLUSIONS

The results obtained with Geant4 simulation for the fields in homogeneous phantoms show an excellent agreement with the measured dose data. All the statistical comparisons state that there is not a statistical difference between the experimental measurements and the data obtained with the Geant4 simulations.

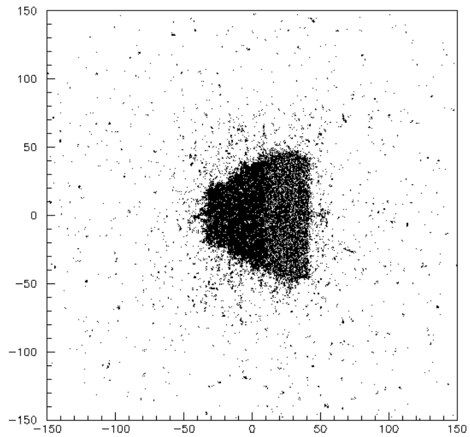

Figure 8: Dose distribution in a plane given by the modulated beam, this distribution was obtained with the simulation system; the dimensions of the symbols in the picture are proportional to the absorbed dose.

This method of dose calculation can be a dosimetry tool in addition to the traditional analytical treatment planning systems.

This simulation can be used, changing some parameters in the model of the geometry, to study also others medical linac's heads. The linac simulation system tool is publicly available with the Geant4 release as an Advanced Example.

5 REFERENCES

1. Geant4 Collaboration, "Geant4 - a simulation toolkit", *NIM A*, **vol. 506**, pp. 250-303 (2003).
2. S. Chauvie, G. Depaola, V. Ivanchenko, F. Longo, P. Nieminen, M.G. Pia, "Geant4 Low Energy Electromagnetic Physics" *Proceedings of CHEP 2001*, Beijing, China, 2001, pp. 337-340 (2001).
3. G. Barrand et al. Abstract Interfaces for Data Analysis - Component Architecture for Data Analysis Tools *Proceedings of CHEP 2001*, Beijing, China, 2001.
4. International Atomic Energy Agency, *Absorbed Dose Determination in External Beam Radiotherapy: An International Code of Practice for Dosimetry Based on Standards of Absorbed Dose to Water*, **Technical Reports Series No. 398**, IAEA, Vienna (2000).
5. G.A.P. Cirrone, S. Donadio, S. Guatelli, A. Mantero, B. Mascialino, S. Parlati M.G. Pia, A. Pfeiffer, A. Ribon, P. Viarengo "A Goodness-of-Fit Statistical Toolkit" *Transactions on Nuclear Science*, **vol. 51 (5)**, pp. 2056-2063 (2004).
6. A.N. Kolmogorov, "Sulla determinazione empirica di una legge di distribuzione", *Giornale dell'istituto italiano degli attuari*, **vol.4**, pp. 83-91 (1933).
7. Gamma, Helm, Johnson, Vlissides, *Design Patterns*, Addison-Wesley